The structure of a working catalyst ; from flat surfaces to nanoparticles

Roobol, S.B.

Chapter 5

NO reduction by H_2 over Pt(110) studied by SXRD

This chapter describes the results of a 144-hour measurement campaign at the ID03 beamline of the ESRF. It was devoted to an exploratory investigation of the surface structure of a Pt(110) single-crystal surface during high-pressure, high-temperature NO and H_2 exposure. Here, we report the two main observations, namely (i) the appearance of a wide variety of surface reconstructions, and (ii) extensive faceting of the surface. The precise conditions under which these effects occur will need to be investigated more systematically in future experiments.

5.1 Introduction

The catalytic conversion of nitrogen oxides (NO_x) is one of the three processes taking place on the three-way car catalyst[84, 85]. This chapter concerns the reaction between nitric oxide (NO) and H_2 over platinum, which is a model reaction for this process. In this case, the formation of nitrogen via

$$2\,NO + 2\,H_2 \longrightarrow N_2 + 2\,H_2O \tag{5.1}$$

leads to the desired, non-toxic reaction products, however the selectivity for this reaction is very low on platinum[86]. Instead, the reactions that lead to the formation of ammonia (NH_3) and nitrous dioxide (N_2O) are dominant. For application as a car catalyst these products need to be avoided, and typically rhodium is added to aid the NO removal.

There have been many UHV studies on the $NO/H_2/Pt$ system. NO adsorbs molecularly on platinum surfaces with the nitrogen atom bound to the surface[87]. The (100) surface binds NO more strongly than the (111) and (110) surfaces, and is also more active for dissociation of the molecule[88]. On the (110) surface, NO lifts the missing-row reconstruction[87]. It preferentially sits on the bridge sites of the atom rows at low coverages and moves to the top sites at high coverages[89–91]. Hydrogen prefers the bridge sites on the (1×2) atomic rows and competes with CO adsorbed on the top sites[92]. When the Pt(100) surface is co-exposed to H_2 and NO, the quasi-hexagonal reconstruction of the clean surface is lifted, depending on the NO coverage[93]. In combination with the difference in turnover rate between the reconstructed and the non-reconstructed surface, this can give rise to kinetic oscillations under certain conditions[94, 95]. As for the high-pressure regime, we have not found any literature on high-pressure surface-science experiments on the reduction of NO by H_2 on Pt(110).

5.2 Methods

The experiment was performed at the ID03 beamline of the ESRF with 18 keV X-rays using the high-pressure Surface X-Ray Diffraction (SXRD) flow reactor[22]. This setup allows UHV sample preparation followed by in-situ high-pressure, high-temperature gas exposure, during SXRD or Grazing Incidence Small Angle X-ray Scattering (GISAXS) measurements simultaneous with reactivity measurements by a quadrupole mass spectrometer.

The Pt(110) sample was cleaned at the beginning of the experiment by repeated cycles of argon ion bombardment and annealing in UHV, resulting in a (1×3) missing-row[96] reconstructed surface, exposing narrow (111) facets (figure 5.1). The (1×3) structure was probably stabilised by carbon segregated from the bulk[97], which was not fully removed because the sample was not annealed in oxygen.

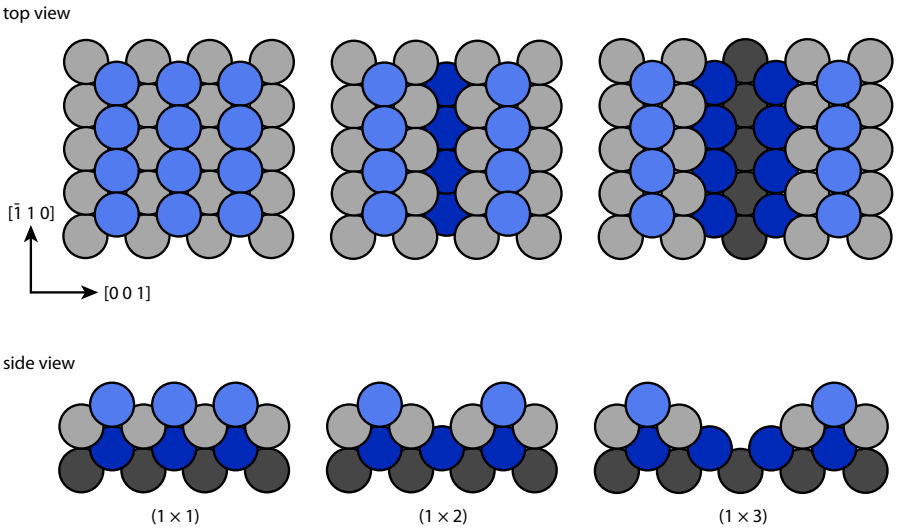

Figure 5.1. Ball models of the surface structure of Pt(110), without a reconstruction (left) and with the (1 × 2) and (1 × 3) missing-row reconstructions (middle and right)[96]. The h-axis of reciprocal space is chosen to correspond to the closed-packed $[\bar{1}10]$ direction and k to the open $[001]$ direction.

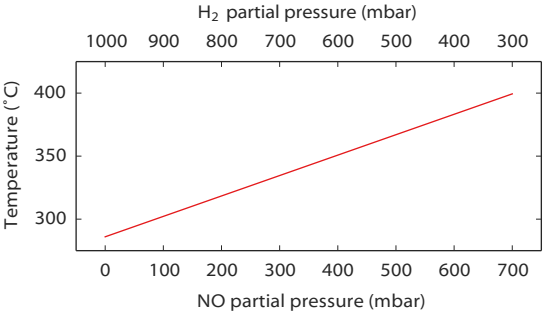

Figure 5.2. Sample temperature as a function of gas composition (mixture of NO and H_2 at 1000 mbar total pressure) for all measurements in this chapter. The sample heater was operated at constant power, but the difference in thermal conductivity between NO and H_2 results in a 100°C temperature difference between the higher and lower H_2 partial pressures used in this experiment.

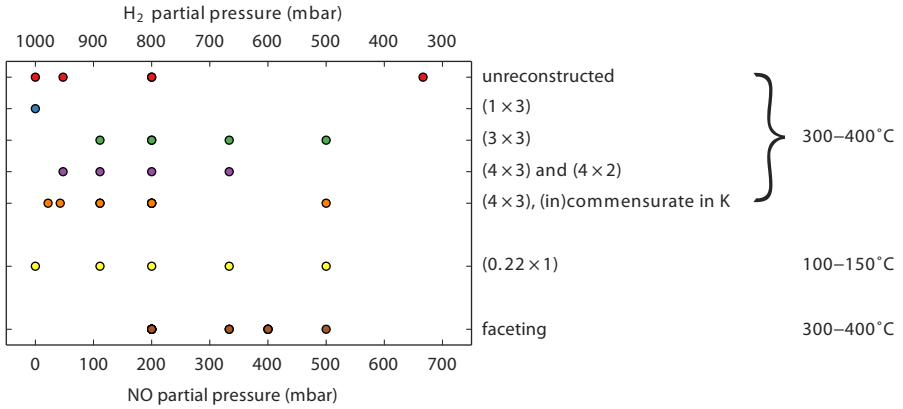

Figure 5.3. Observed reconstructions (periodicities) on Pt(110) as a function of gas composition (mixture of NO and H_2 at 1000 mbar total pressure). The sample temperature was in the range 300–400°C and can be found in figure 5.2, except for the "0.22" reconstruction which has been observed at approximately 100–150°C. The faceting always coincided with the presence of the (in)commensurate (4 × 3) reconstruction and is analysed in detail in figures 5.8–5.11. Figure 5.4 shows the scans along *h* and *k* corresponding to the reconstructions.

During high-pressure exposure the sample was heated at constant power, resulting in a temperature of 300–400°C depending on the gas composition (figure 5.2). At these temperatures, the ammonia production is problematic, with the ammonia signal in the mass spectrometer rising to values corresponding to tens of mbar in the reactor. Due to the low pumping speed for these molecules it was not possible to keep their partial pressures at a constant and low level throughout the experiment. Since these molecules also affected the leak rate of gas from the reactor to the mass spectrometer, and eventually completely inhibited the leak, their presence could not be monitored with any accuracy during the experiment. In addition, as the experiment progressed, the UHV pressure deteriorated, at some stage making it impossible to perform further sputter/anneal cycles to regain a clean sample.

5.3 Results and discussion

Many different surface structures have been observed on the platinum surface depending on the conditions. They can be classified in two groups: surface reconstructions, requiring modest rearrangement of platinum atoms, and faceting, corresponding to massive material transport along the platinum surface.

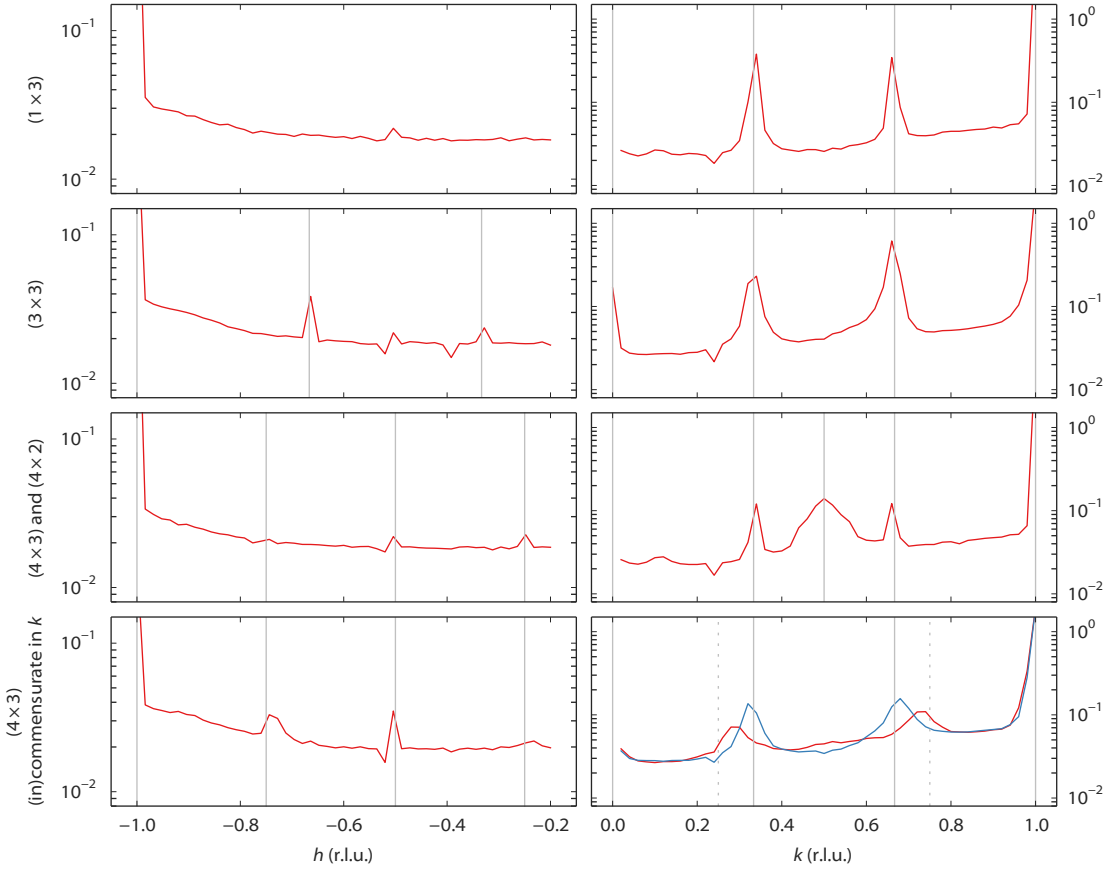

Figure 5.4. Observed reconstructions on the Pt(110) single crystal surface. See figure 5.3 for the conditions. Left column contains scans along $[h\,0\,0.5]$ in reciprocal lattice units (r.l.u.), right column along $[-1\,k\,0.3]$. The y-axes show intensity in arbitrary units. The solid vertical lines indicate the periodicity of the pattern. The lower right panel shows an incommensurate periodicity (red) that becomes commensurate (4 × 3) with time (blue). The dotted vertical lines mark $k = 0.25$ and $k = 0.75$.

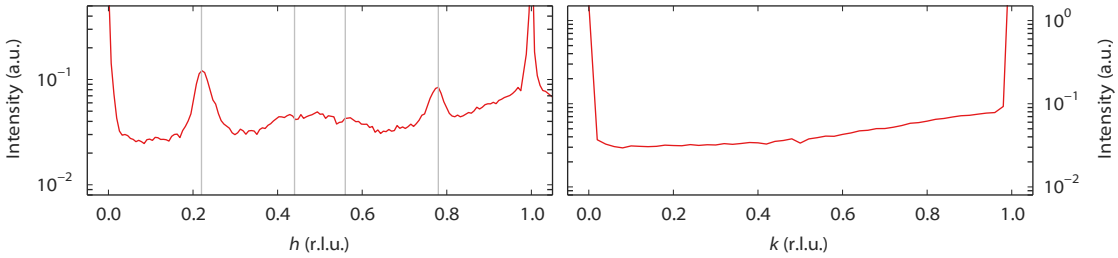

Figure 5.5. The "0.22" reconstruction observed at 100-150°C (see figure 5.3 for the gas composition where this reconstruction occurs). Left panel contains a scan along $[h\,1\,0.3]$, right panel along $[-1\,k\,0.3]$. There are peaks at 0.22 r.l.u. from the Bragg peaks along the h-direction, and a hint of the second order peaks as well, as indicated by the vertical lines in the left panel.

5.3.1 Surface reconstructions

When the partial pressures of NO and H_2 are varied, several reconstructions of the Pt(110) surface have been observed at 1 bar total pressure and at 300–400°C. Figures 5.3 and 5.4 indicate the appearance of the (1×3), (3×3), (4×3) periodicities plus some variations. At lower temperatures (100–150°C), another reconstruction appeared (figure 5.5), with peaks at 0.22 reciprocal lattice units (r.l.u.)[1] away from the Bragg peaks in the h-direction.

The (1×3) reconstruction observed in H_2 is likely the same missing-row reconstruction observed on the freshly prepared sample, but all the others have not been identified before. Few $(n \times 2)$ and $(n \times 3)$ reconstructions of (110) surfaces, formed under the influence of adsorbates at low pressures, have been reported, and they differ considerably in character. The H-induced (5×2) structure on Ni(110) consists of a zigzag pattern formed by short (2 atoms long), alternating pairings of the atom rows[98]. On the other hand, the O-induced c(6×2) structure on Cu(110) consists of a checkerboard-pattern of isolated copper atoms decorated by oxygen[99]. In this structure, the occupancy of metal atoms in the two upper layers is much lower than in the unreconstructed surface and there are no closed-packed rows. Finally, two N-induced (2×3) structures on Cu(110) are of the missing-row type[100], having one every three atom rows missing in the upper layer. These two structures differ by the number and position of the nitrogen atoms in the (2×3) unit cell. The l-scans along the superstructure rods of the (3×3) reconstruction

[1] In SXRD, the directions in reciprocal space are labeled by h, k and l, and coordinates are usually given in units of the basis vectors of the reciprocal lattice (i.e. reciprocal lattice units or r.l.u.). This concept is closely related to the Miller indices used to label lattice planes in crystals. For simple crystals, this ensures that Bragg peaks always have integer coordinates. By convention, the h and k directions are parallel to the surface, whereas the l direction is perpendicular to the surface and points outwards. See also figure 5.1 for the precise choice of h and k for a (110) surface.

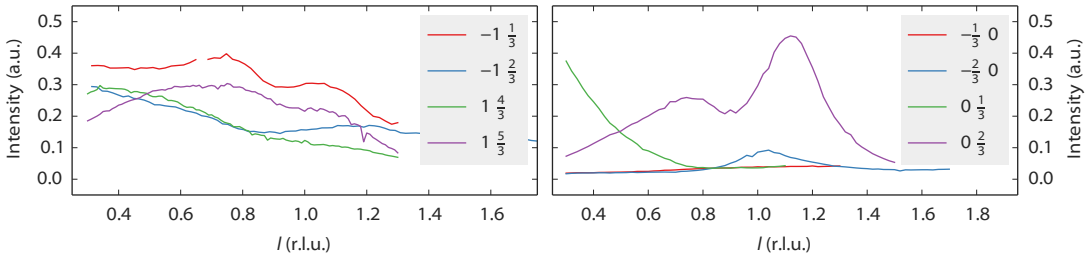

Figure 5.6. l-scans along some superstructure rods. The legends show the h and k values of each scan. The left panel shows the (1 × 3) reconstruction in UHV, with periodicities in l similar to those reported for the (1 × 3) missing row reconstruction by Robinson and co-workers[97]. The right panel shows the (3 × 3) reconstruction in a mixture of 200 mbar NO and 800 mbar H_2 at 320°C. A comparison with the left panel and the data from Robinson suggest that the (3 × 3) is a (1 × 3) missing row with additional periodic structure along the atom rows.

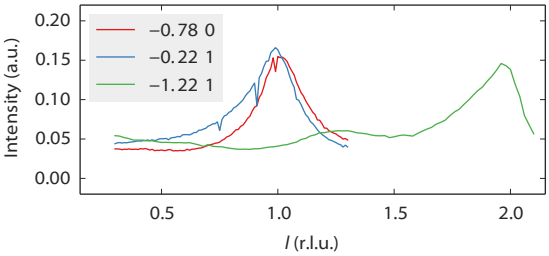

Figure 5.7. l-scans along the superstructure rods for the "0.22" reconstruction, taken at 150°C in pure NO at a total pressure of 200 mbar. The legend shows the h and k values of each scan. The intensity peaks strongly at integer l-values, meaning that the periodicity matches that of the bulk Pt lattice, suggesting that the reconstruction is some structure of Pt.

observed in our experiments (figure 5.6) suggest that it is a variation on the (1 × 3) missing row structure, with additional periodicity along the atom rows.

We have observed the incommensurate (4 × 3) structure on several occasions and it always transformed into a commensurate (4 × 3) structure with time. The incommensurability could be due to mixtures of (4 × 4) and (4 × 3) structures. Similar effects have been reported for variable fractions of (1 × 2), (1 × 3) and (1 × 5) missing-row reconstructions on Pt(110) induced by C segregation[101], and also for mixtures of (1 × 2) and (1 × 3) missing-row reconstructions of H- or Au-covered Pd surfaces[102, 103]. No l-scans have been obtained for the (4 × 3)-related structures, however, we suggest it could also be a variation on the (1 × 3) missing row. The "0.22" reconstruction, which is also incommensurate, seems to be completely different. It appears to be completely stable in time, and l-scans (figure 5.7) suggest that the

intensity derives from a significant restructuring of the Pt surface rather than an adsorbate overlayer pattern, but a more detailed structure analysis has not been performed.

As figure 5.3 indicates, there is no clear separation between the different structures as a function of gas composition. For the clean Pt(110) surface it is known that the free energies of the various $(1 \times n)$ missing-row reconstructions are very similar[104], with the consequence that small changes in conditions (for example the presence of small amounts of adsorbates from the gas phase or segregated impurities from the bulk) can easily push the system from one phase into another. A similar mechanism could be at play for the variety of reconstructions observed here, under high-pressure, high-temperature conditions.

5.3.2 Faceting

Near the end of the experiment, under conditions already probed before in this measurement session, the surface started faceting (see figure 5.3 for the conditions). This was observed by taking two-dimensional cuts perpendicular through a crystal truncation rod (CTR). A CTR is a scan along l connecting Bragg peaks of the crystal. Its shape is defined by the crystal termination, i.e. the precise configuration of atoms in the transition from the regular lattice in the crystal bulk to the empty space above it (vacuum or gas phase)[105]. The profile of a cut through the CTR contains information on the height variations on the surface. In our case, the two-dimensional cuts were constructed from a collection of continuous scans along the diffractometer angle ω[68] that were stitched together using *BINoculars* (chapter 4). The cuts in figure 5.8 reveal the appearance of satellite peaks, whose distance to the main peak is proportional to the distance Δl to the nearest Bragg peak. In other words, the extra peaks correspond to extra CTRs, tilted with respect to the $[110]$ normal of the average surface. Indeed, sufficiently well-defined facets will give rise to an extra set of tilted truncation rods through every Bragg peak, as explained in figure 5.9. The angle of these facet rods directly corresponds to that of the surface normal of the facet. The full width at half maximum (FWHM) then gives a measure for the definition of the facet. The faceting angle was determined by a fitting procedure (figure 5.10) of which the combined results are shown in figure 5.11.

The facets are tilted by 8 to 12 degrees away from the (110) surface in the $[\bar{1}\,1\,0]$ direction. The facet angle seems to be negatively correlated to the NO partial pressure, higher NO pressures resulting in smaller angles. Figure 5.11 also suggest that not all data points have been taken with the system in equilibrium. Especially for NO partial pressures above 300 mbar, the right panels indicate the response to be slow, on the time scale of the measurements. The FWHM of the CTR is a measure for the roughness of the crystal surface, and this shows, as expected, a clear

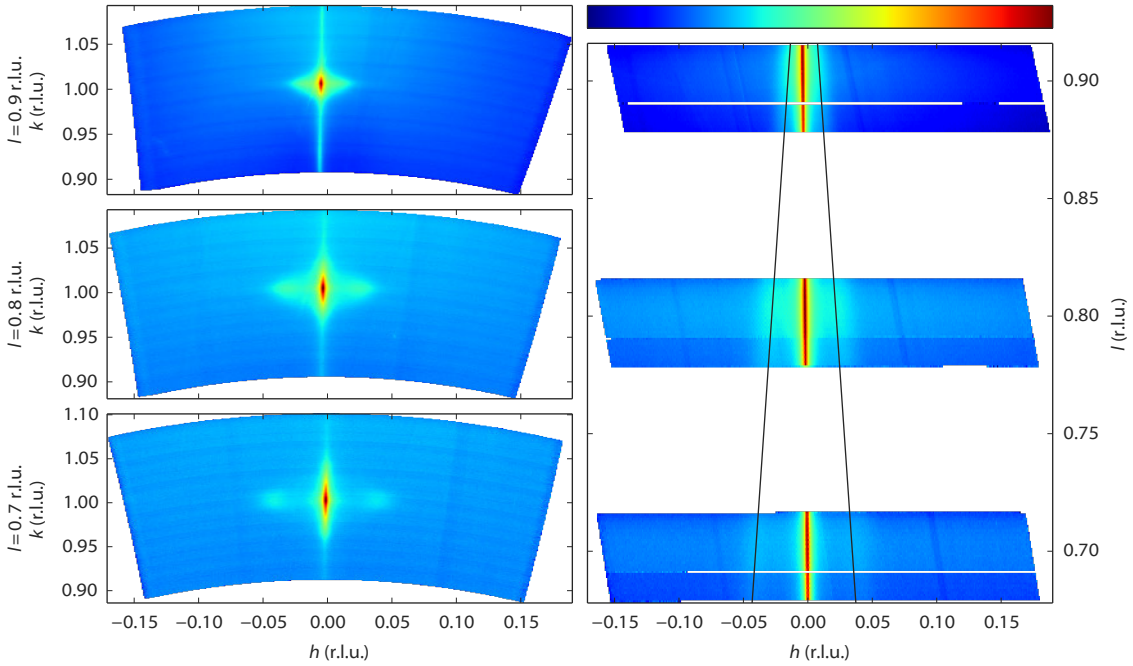

Figure 5.8. Faceting of the Pt(110) surface has caused the appearance of satellite peaks close to the crystal truncation rods (CTRs). The left panels show three (hk)-cuts at constant l, intersecting the $(1\,0\,l)$ CTR at three values of l, obtained during exposure to a mixture of 400 mbar NO and 600 mbar H_2 at 350°C. The right panel is a projection of a subset of these data onto the hl plane, showing that the satellite peaks line up into two tilted CTRs that pass through the Bragg peak at $l = 1$. Therefore they can be interpreted as the CTRs of two sets of well-defined facets, and their directions correspond to the surface normals of the facets. The intensity ranges corresponding to the logarithmic colour scale (shown above the right panel) are for the lefts panel, from top to bottom, $[9.4 \cdot 10^{-6}, 1.7 \cdot 10^{-1}]$, $[3.0 \cdot 10^{-6}, 1.8 \cdot 10^{-2}]$, $[2.6 \cdot 10^{-6}, 5.1 \cdot 10^{-3}]$, and for the right panel, from top to bottom, $[3.1 \cdot 10^{-5}, 2.4 \cdot 10^{-2}]$, $[6.7 \cdot 10^{-6}, 4.4 \cdot 10^{-3}]$, $[5.7 \cdot 10^{-6}, 1.9 \cdot 10^{-3}]$.

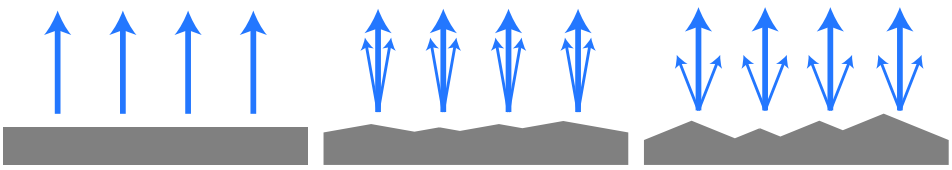

Figure 5.9. The surface termination of a flat surface gives rise to crystal truncation rods (CTRs) along the surface normal (left panel). The presence of facets on the surface results in the appearance of titled truncation rods (middle and right panel).

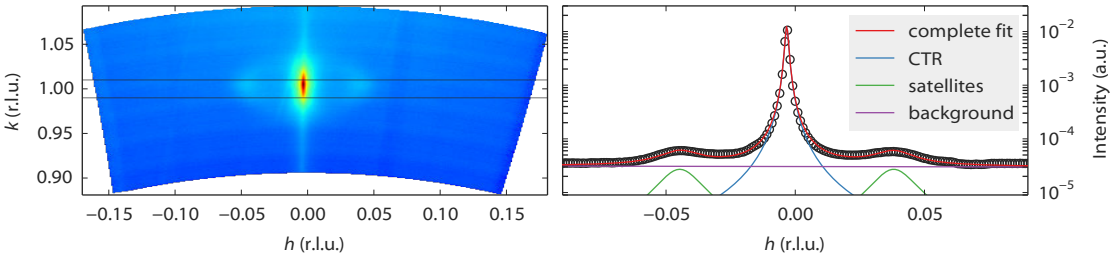

Figure 5.10. The region indicated in the left panel was used to further analyse the faceting. The position of the satellite peaks has been fitted using a least-squares optimization of three Lorentzians plus a sloped background. The satellite peaks were assumed to be symmetrically positioned on either side of the rod, and to have identical peak widths.

correlation with the faceting angle. The FWHM of the facet rods took some time to reach a constant value, indicating that the facets were growing in average size, at least until measurement 10, which was acquired 4 hours after measurement 1.

The tilt of approximately 10° implies that the facets typically have the (320) structure (figure 5.12), a crystal plane that makes an 11.3° angle with the (110) plane. The higher index orientations (430) and (540), having a similar structure as (320) but with 4 and 5 atoms per terrace and tilts of 8.1 and 6.3° respectively, are likely to be present as well, especially at higher NO pressures.

Faceting of the Pt(110) into mainly (320) has been observed with CO and O_2 exposure in the 10^{-4} mbar regime[106, 107]. In this case, the presence of both reactants is required to create the facets, and the mechanism is suggested to be related to the strong binding of oxygen on step sites, and material transport induced by switching between the (1×2) missing row reconstruction and the unreconstructed surface due to CO coverage fluctuations. The reactivity of the (320) plane is higher than that of the (110) plane and under some conditions this gives rise to kinetic oscillations[108].

In the case of the NO and H_2 exposure, a comparable mechanism could be responsible for the faceting, causing the free energy of the (320) and similar orientations to reach a lower value than the free energy of the (110) surface. As in the case of CO and O_2 exposure, it could be due to an adsorbate binding strongly to the steps, and in this case NO, H_2O, NH_3, or atomic oxygen are likely candidates.

However, there is an alternative explanation that is supported by DFT calculations by Reuter and co-workers[109]. They show that the surface stress of a Pt(110) surface is dramatically influenced by adsorbed NO molecules due to the strong repulsive interaction between NO molecules at higher coverages. Their calculations show that the surface stress in the $[1\bar{1}0]$-direction changes from 3.0 N/m (tensile) for the clean surface to -3.0 N/m (compressive) for a 1 ML coverage of NO. The change along the [0 0 1]-direction is less dramatic, the surface stress being -0.2 N/m

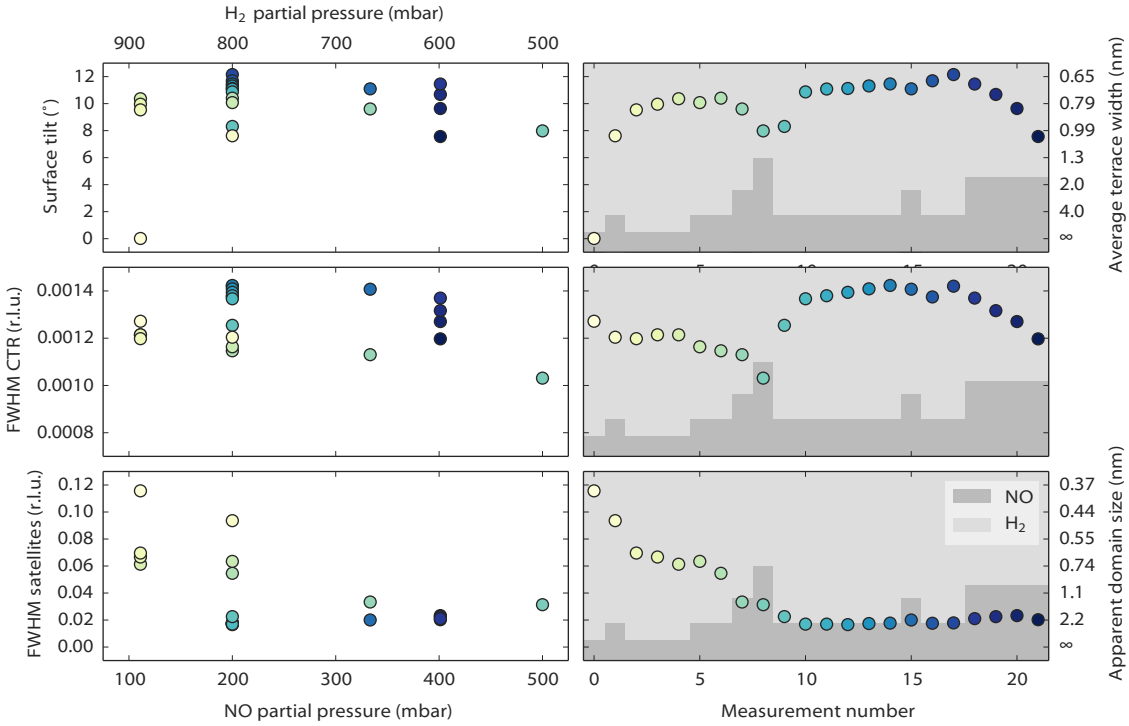

Figure 5.11. Combined results of the fitting procedure described in figure 5.10. The panels on the left represent fit parameters as a function of gas composition (NO and H_2 mixtures at a total pressure of 1 bar), the panels on the right show the same parameters as a function of measurement number, with the fractional gas composition indicated by the shades of grey in the background. See figure 5.2 for the sample temperature. The upper panels contain the angle of the surface normal of the facets and the corresponding terrace width (right axis), which is calculated from the position of the satellite peaks. The middle panels correspond to the full width at half maximum (FWHM) of the main rod, while the lower panels show the FWHM of the facet rods, both in reciprocal lattice units (r.l.u.). For the satellite peaks the FWHM has been converted into the apparent domain size (right axis). This calculation is only valid in the unlikely case that no other effects contribute to the FWHM, and must therefore be considered a lower bound for the domain size.

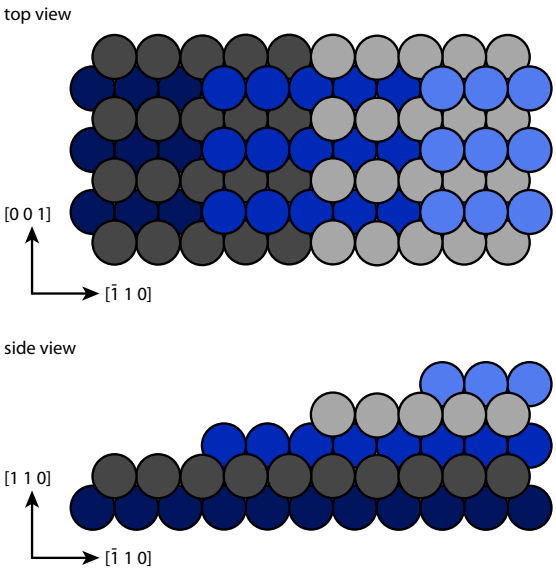

Figure 5.12. Ball model of the stepped Pt(320) surface having its surface normal titled 11.3° away from the [110] orientation.

for the clean surface and 1.4 N/m for the NO covered surface. Within the accuracy of the DFT calculations, the chemical potential required for 1 ML NO coverage matches that of the high-pressure, high-temperature NO exposure described in this chapter. The faceting in the $[1\bar{1}0]$-direction could be a way for the surface to cope with a large change in surface stress in this direction. This concept is supported by literature. Hanesch and co-workers report morphology changes on mesoscopic length scales of Pt(110) surfaces induced by surface stress[110]. Adsorbate-induced surface stress has been measured on Ni surfaces, in particular for CO on Ni(100) and (111)[111], and for various atomic species on Ni(100)[112]. Given the fact that the DFT calculations show a large change in stress in the direction where the faceting occurs, we suggest that the NO-induced surface stress drives the faceting, rather than enhanced NO adsorption at steps.

5.4 Outlook

Pt(110) shows a variety of surface structures during exposure to mixtures of NO and H_2. The appearance of many reconstructions indicates the sensitivity of the surface to adsorbates. The precise conditions leading to each of the observed reconstructions warrant further investigation. Combining surface X-ray diffraction with a real-space microscopy technique such as STM should make it easier to determine the structural

details of the observed reconstructions. For a next round of experiments it would be preferable to start with the proper (1×2) missing-row reconstruction of the genuinely clean Pt(110) surface. This requires annealing the Pt sample in O_2. In addition, it would be better to set the gas composition and temperature independently. Longer waiting times (in the order of hours) at each set of conditions are also necessary to ensure that the observed structures reflect true equilibrium. In addition, the presence of the ammonia needs to be avoided or suppressed, or its role should be studied systematically.

For the faceting it is important to understand why it only occurred after prolonged exposure, near the end of the experiment, and not earlier when the same conditions where applied to the sample. Possible explanations could be (again) the presence of ammonia or a contaminant from the crystal bulk or the gas phase. DFT calculations on stepped Pt(110) surfaces could provide the definitive answer to the mechanism driving the faceting, but calculations on stepped surfaces are still challenging due to the large unit cell required. In addition, the influence of the facets on the activity and selectivity of the Pt(110) surface for NO reduction by H_2 is a relevant topic for further work, both experimentally and using DFT.

Apart from these suggestions for follow-up experiments, there is another, perhaps even more challenging direction, in which research on the interaction of NO with platinum should proceed, namely to go beyond flat surfaces and study the effect of NO and H_2 on supported nanoparticles, a more realistic model catalyst. The next chapter describes this step.